Available online at www.sciencedirect.com
SCIENCE DIRECT®
C. R. Mecanique 331 (2003) 515–523
COMPTES RENDUS MECANIQUE

Mixing is an aggregation process

Emmanuel Villermaux [a], Jérôme Duplat [b]

[a] *Université de Provence & institut universitaire de France, IRPHE, 13384 Marseille cedex 13, France*
[b] *Université de Provence, IUSTI, 13453 Marseille cedex 13, France*

Received 24 February 2003; accepted after revision 8 April 2003

Presented by Paul Clavin

Abstract

With the aid of several demonstration experiments, it is shown how a stirred scalar mixture relaxes towards uniformity through an aggregation process. The elementary bricks are stretched sheets whose rates of diffusive smoothing and coalescence build up the overall mixture concentration distribution. The cases studied, in particular, include mixtures in two and three dimensions, with different stirring protocols, which all lead to a family of concentration distributions stable by self-convolution. ***To cite this article: E. Villermaux, J. Duplat, C. R. Mecanique 331 (2003).***

Résumé

Le mélange est un processus d'agrégation. Des expériences démonstratives suggèrent qu'un mélange scalaire agité relaxe vers l'uniformité à travers un processus d'agrégation. Les briques élémentaires sont des feuillets étirés qui se diluent dans le milieu en même temps qu'ils s'agrègent, construisant par là l'ensemble de la distribution de concentration de la mixture. Les cas considérés en particulier sont des mélanges en deux et trois dimensions, agités par des protocles très différents et qui pourtant donnent naissance aux mêmes distributions de concentration, stables par auto-convolution. ***Pour citer cet article : E. Villermaux, J. Duplat, C. R. Mecanique 331 (2003).***

Keywords: Turbulence; Mixing; Stirring; Diffusion; Aggregation

Mots-clés : Turbulence ; Mélange ; Agitation ; Diffusion ; Agrégation

Version française abrégée

Dans son traité sur la *Théorie Analytique de la Chaleur* de 1822, Joseph Fourier [1] découvre que « le principe de la communication de la chaleur » consiste en l'échange de chaleur entre « molécules » voisines lorsque celles-ci sont portées à des températures différentes. La quantité de chaleur échangée est proportionnelle à l'écart entre les températures, et ne dépend pas de leur valeur absolue : la linéarité du processus de diffusion est établie. On sait en

E-mail address: villerma@irphe.univ-mrs.fr (E. Villermaux).

1631-0721/$ – see front matter
doi:10.1016/S1631-0721(03)00110-4

conséquence qu'on peut reconstituer le champ de concentration $C(x,t)$ d'une substance qui diffuse (de manière analogue à la chaleur) depuis son profil initial, $C(x,0)$ par

$$C(x,t) = \int \frac{\mathrm{e}^{-(x-x')^2/(4Dt)}}{2\sqrt{\pi Dt}} C(x',0)\,\mathrm{d}x' \tag{1}$$

cette relation exprimant la *somme* des profils de concentration élémentaires pondérée par leur poids initial $C(x',0)\,\mathrm{d}x'$.

L'interprétation faite des expériences présentées dans cet article tire parti de la propriété d'addition des concentrations élémentaires pour le mécanisme de construction de la densité de probabilité $P(C)$ des concentrations dans un milieu agité. En effet, imaginons qu'on trouve dans un milieu le niveau de concentration C_1 avec la probabilité $P_1(C_1)$ en provenance d'une source 1, et le niveau de concentration C_2 avec la probabilité $P_2(C_2)$ en provenance d'une source 2. Si les particules fluides portant ces niveaux de concentration se rapprochent au même point de l'espace, fusionnent leur profils de concentration, et que le milieu est agité de manière suffisamment aléatoire pour que ces concentrations soient choisies indépendamment dans chacune des distributions sources, alors la probabilité $P(C)$ de trouver un niveau de concentration C en ce point de l'espace sera

$$P(C) = \int_0^C P_1(C_1)P_2(C_2)\,\mathrm{d}C_1, \quad \text{avec } C = C_1 + C_2 \tag{2}$$

L'opération ci-dessus définit une *convolution* entre les distributions sources. Nous montrons plus bas que cette remarque est utile pour comprendre la forme et l'évolution des distributions sources elles-mêmes puisque les niveaux de concentration interagissent entre eux dans une mixture agitée. Les distributions de concentration résultantes se trouvent être stables vis-à-vis du processus qui leur donne naissance, c'est-à-dire un processus d'agrégation, d'addition locale, dont le pendant dans le domaine des densités de probabilité est un processus d'auto-convolution.

A mixture is a transient state between the initial segregation of the constituents, and their ultimate homogeneity. The overall mixing process of a drop of dyed fluid in a stirred medium involves two phenomena: a process of dispersion of the drop in the diluting medium by which the phases interpenetrate, and a process of interaction between the dispersed elements from which homogeneity arises. We report on findings suggesting that the nature of the interaction is of an aggregation type.

Let a jet of water plus a diluted fluorescent dye (disodium fluorecein) discharge in a square, transparent, long duct. For a given duct cross section, the injection diameter d and the velocity of the co-flow at the entrance of the duct can be varied so that the average concentration of the dye in the channel $\langle C\rangle$ can be set at will. Since the cross-section of the duct and the average velocity of the mixture in the downstream direction are constant, the average concentration is constant as well. The jet velocity u is such that the Reynolds number $Re = ud/\nu \simeq 10^4$, where ν denotes the fluid kinematic viscosity.

The flow is visualized by means of a plane Argon laser sheet slicing the duct along its axis, and as can be seen on Fig. 1, the dye rapidly invades the whole duct cross section, erasing its concentration differences as it travels downstream to relax towards a more or less uniform mixture.

After the dye has filled the channel cross section and evolves around a constant average concentration, the distribution $P(C)$ presents a skewed, bell shape which gets narrower around $\langle C\rangle$ in time (axial distances are converted to time through the average axial velocity with confidence as the radial velocity profile in a turbulent duct is flat [2]). The shape of $P(C)$ is very well described by a family of one parameter distributions, namely Gamma distributions

$$P(X) = \frac{n^n}{\Gamma(n)} X^{n-1}\,\mathrm{e}^{-nX}, \quad \text{where } X = \frac{C}{\langle C\rangle} \tag{3}$$

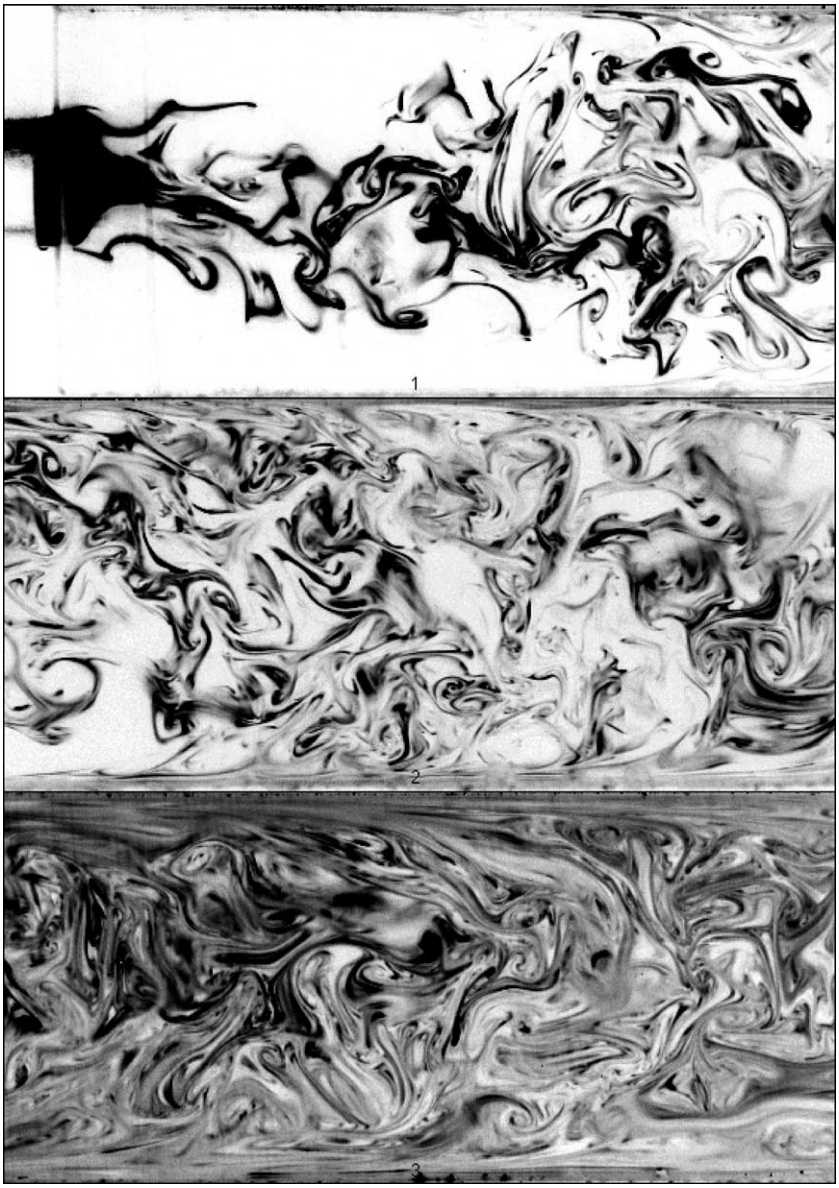

Fig. 1. Mixing of a dye discharging from a jet of diameter $d = 8$ mm in a square ($L \times L$ with $L = 3$ cm) duct. From 1 to 3, successive instantaneous planar cuts of the scalar field at increasing downstream locations in the duct showing the progressive uniformization of the dye concentration.

Fig. 1. États de mélange successifs d'un colorant passif dans un canal turbulent.

The parameter n is adjusted at each downstream location for the Gamma distribution of Eq. (3) to fit the experimental one. It is seen on Fig. 2 that the fairness of the fit holds for the whole concentration range, down to quite low probability levels, and accounts for the downstream deformation of $P(C)$ through the single parameter n, whose dependence on the downstream location is quite strong: Fig. 2 suggests a power-law dependence with an exponent close to $5/2$. The dependence of n on the jet Reynolds number is, although noticeable, very weak.

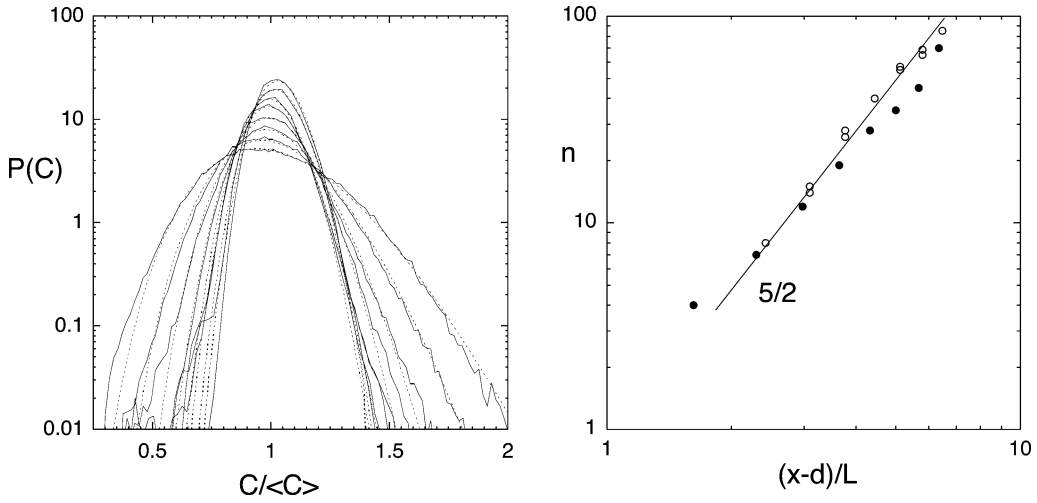

Fig. 2. Left: Downstream evolution of the concentration distribution $P(C)$ as the dye progresses along the duct as shown on Fig. 1. The concentration distribution of the evolving mixture gets narrower around the average concentration $\langle C\rangle = 0.3$. Solid line: experimental distributions, dashed line: distributions given by Eq. (3). Right: Fitting parameter n of the distributions (3) as a function of the downstream distance $(x-d)/L$. ∘: $Re = 10^4$, •: $Re = 5\times 10^3$.

Fig. 2. Distributions de concentration pour des distances successives à l'aval dans le canal et ajustement par les distributions données par l'Éq. (3). Évolution du paramètre d'ajustement n avec la distance aval.

The stirring motions progressively convert a compact blob in a set of sheets of increasing surface and decreasing thickness [3,4]. The intersects of these sheets with the visualization plane are visible on Fig. 1 in the form of ligaments. Let $s(t)$ be the distance between two material particles in the direction z perpendicular to a sheet, and $\sigma(t) = \partial \ln s(t)/\partial t$ its rate of compression. If $c(z,t)$ is the scalar concentration profile across the sheet, the convection–diffusion transport equation reduces to a one-dimensional problem provided the radius of curvature of the sheet is large compared to its thickness [5]. In that case the direction z aligns with the direction of maximal compression and for a species with diffusion coefficient D

$$\frac{\partial c(z,t)}{\partial t} + \sigma(t) z \frac{\partial c(z,t)}{\partial z} = D\frac{\partial^2 c(z,t)}{\partial z^2} \tag{4}$$

By the change of variables $\tau = D\int_0^t \mathrm{d}t'/s(t')^2$ and $\xi = z/s(t)$, Eq. (4) reduces [6–8] to a simple diffusion equation $\partial c(\xi,\tau)/\partial\tau = \partial^2 c(\xi,\tau)/\partial\xi^2$. The topology of the stirring motions select particular forms for $s(t)$. Starting with a sheet of initial uniform concentration and thickness s_0, the maximal concentration in $z = 0$ can be written

$$c(0,t) = \operatorname{erf}\left(1/4\sqrt{\tau}\right) \tag{5}$$

We describe several generic examples: in incompressible flows in two dimensions where the length of material lines grow like γt, the mean transverse thickness of the scalar filaments decrease as $s(t) = s_0/\sqrt{1+(\gamma t)^2}$ and thus $\tau = \frac{Dt}{s_0^2}(1 + \frac{(\gamma t)^2}{3})$, providing $c(0,t) \sim (t/t_s)^{-3/2}$ for $t > t_s$, with $t_s \sim \frac{1}{\gamma}Pe^{1/3}$, where $Pe = \gamma s_0^2/D$ is a Péclet number. If material surfaces in three dimensions grow like $(\gamma t)^2$, then [9], $s(t) = s_0/(1+(\gamma t)^2)$ and $\tau = \frac{Dt}{s_0^2}(1 + \frac{2}{3}(\gamma t)^2 + \frac{1}{5}(\gamma t)^4)$, providing $c(0,t) \sim (t/t_s)^{-5/2}$ for $t > t_s$, with $t_s \sim \frac{1}{\gamma}Pe^{1/5}$. For flows in which the length of material lines increases exponentially in time like $\mathrm{e}^{\gamma t}$ as realized by a succession of stretching and folding motions in random flows [10], $s(t) = s_0\,\mathrm{e}^{-\gamma t}$ and $\tau = \frac{Dt}{s_0^2}(\mathrm{e}^{2\gamma t} - 1)$ providing $c(0,t) \sim \mathrm{e}^{-\gamma t}$ for $t > t_s$ with $t_s \sim \frac{1}{2\gamma}\ln Pe$. These timescales are the relevant mixing times as soon as the inverse of the elongation rate γ^{-1} is

smaller than the diffusive time of the sheet constructed on its initial size s_0^2/D, that is for $Pe \gg 1$. In this limit, t_s is essentially given by the time needed to deform the sheet γ^{-1} and pure diffusion (for which $c(0,t) \sim (Dt/s_0^2)^{-1/2}$) is enhanced by the substrate motion.

However, the sheets interact as they move in the flow so that their diffusive boundaries interpenetrate to give rise to new sheets whose concentration profile is the *addition* of the original ones. This elementary interaction rule is a consequence of the linearity of the Fourier [1] diffusion equation (3) and this coalescence process explains why, although the concentration of each individual element $c \equiv c(0,t)$ decreases in time according to Eq. (5), the average concentration $\langle C \rangle$ is conserved. Because of the irregular stirring motions, the addition of the concentration levels is made at random among those available in the population $P(C)$ at time t which therefore evolves by self-convolution as

$$\frac{\partial P}{\partial t} = -\frac{\partial}{\partial C}\left(\left\langle \frac{\mathrm{d}c}{\mathrm{d}t}\right\rangle P\right) + \frac{\mathrm{d}n}{\mathrm{d}t}\left(-P + P^{\otimes(1+1/n)}\right) \tag{6}$$

The first Liouville transport term in Eq. (6) accounts for the decrease of the individual concentration levels given by Eq. (5). This term results in a global shift of the distribution towards the low concentration levels at a rate prescribed by Eq. (5), but does not alter the *shape* of $P(C)$. The second term is the convolution interaction kernel which is responsible for the change in shape of $P(C)$. It originates from $P(C, t+\Delta t) = P^{\otimes(1+1/n)}$ with $1/\Delta t = \mathrm{d}n/\mathrm{d}t$. The non-integer convolution order $1+1/n$ is the continuation of the standard integer convolution in the Laplace space, as can be seen by taking the Laplace transform of Eq. (6). The asymptotic solution of Eq. (6) is, irrespective of the initial condition for $P(C)$, a Gamma distribution of order n.

The average concentration of the mixture a result of the relative weight of these two terms and is not, in general, constant. The piling-up of the concentration levels by coalescence contributes, through the second term of Eq. (6), to the increase of the average concentration by a factor given by $\exp\{\int \mathrm{d}n/n\} = n$. The average concentration is thus conserved if the damping factor of Eq. (5) balances exactly the coalescence rate that is when

$$n = \frac{1}{c(0,t)} \tag{7}$$

The above condition is realized provided $n = 1/c(0,t) \sim (t/t_s)^{5/2}$, as expected in this three-dimensional flow (Fig. 2). Note that this apparent power law is a transient effect reflecting the fact that the temporal window of the mixture's evolution covers, at most, a few large scale turnover time $\gamma^{-1} \sim L/u'$. Indeed, material lines increase like $L/L_0 = \exp(\gamma t) = \exp(u't/L) = \exp(u'/u \times x/L)$ where $x = ut$ is the distance from the injection point of the scalar blob in the medium advected at a velocity u. In the channel flow, the turbulence intensity is such that [2] $u'/u \approx 0.08$ and the downstream distances of observation in the present experiments are such that $x/L < 10$ so that $L/L_0 \approx 1 + u'/u \times x/L = 1 + \gamma t$, realizing in practice an elongation linear in times, inducing, in this three-dimensional flow, $n \sim t^{5/2}$. This behavior has thus to be understood as the birth of the ultimate exponential regime, but this slight difference, if any, has strictly no consequence on the mechanism building-up the concentration distribution $P(C)$ which solely relies on *random additions* of concentration levels, independently of the *rate* at which these additions are made.

By changing the dimensionality of the flow from three to two, one might expect that as long as the stirring motions are sufficiently irregular to ensure an addition of the concentration levels at random, the distribution is, as in the three-dimensional case, generated by self-convolution. It is, by contrast, also expected that the dependence of n on time will be different. We illustrate this difference on hand of a simple experiment consisting in stirring a blob of dye with a rod in a thin layer of a very viscous fluid, by a two-dimensional quasi-periodic protocol which mimics the motion of a straw in a milk shake. The dilluting fluid is pure Glycerol and the drop is made of the same fluid coloured with Indian Ink. A number of parallel cuts is made in one direction, and then the same number at right angle, this operation defining one cycle (Fig. 3).

In this low Reynolds number flow (the typical Reynolds number of the motion of the rod is $Re = us_0/\nu = 10^{-1}$), the fluid is deformed by the passage of the rod on a scale which is given by its own size s_0. The length of material

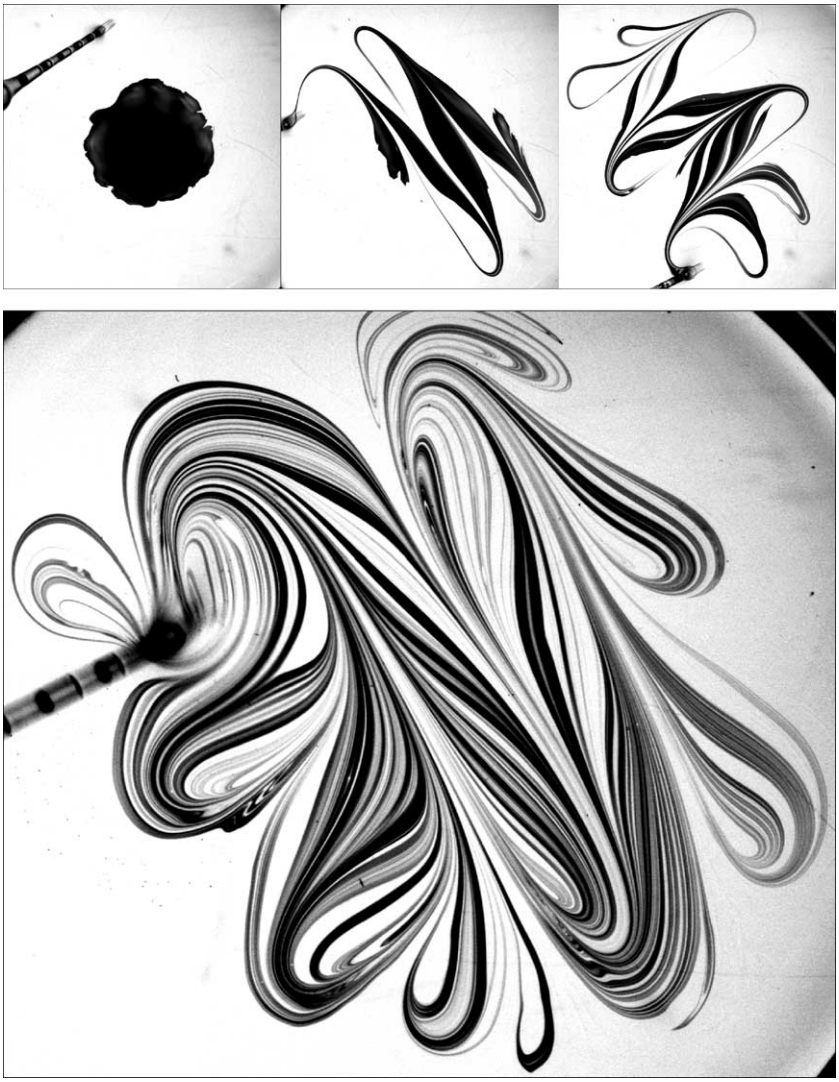

Fig. 3. Top: The stirring protocol of a drop of ink deposed at the surface of pure Glycerol using a small rod. The sequence displays the initial state, half, and a completed stirring cycle. Bottom: the mixture's state after $2\frac{1}{2}$ completed stirring cycles.

Fig. 3. Protocole de mélange d'une goutte colorée dans une couche mince de liquide visqueux.

lines is equal to the distance traveled by the rod in the medium, and it is actually observed that the net contour length of the deformed scalar drop increases in proportion to the number of cycles as

$$L/L_0 = 1 + \gamma t \approx 1 + 17.5 \times p \tag{8}$$

as shown on Fig. 4. The mixing time, or, alternatively, the number of cycles p needed to start mixing the drop in the surrounding medium is thus given by

$$\gamma t_s \approx 17.5 \times p_s \sim \left(\gamma s_0^2/D\right)^{1/3} = (ReSc)^{1/3} \tag{9}$$

With $\gamma \approx u/s_0$ the typical elongation rate, $u \approx 4.6$ cm/s the rod velocity, Eq. (9) gives, with $s_0 \approx 2$ mm and $Sc \approx 10^6$, a mixing cycle p_s of the order of 2.5 (see Fig. 4).

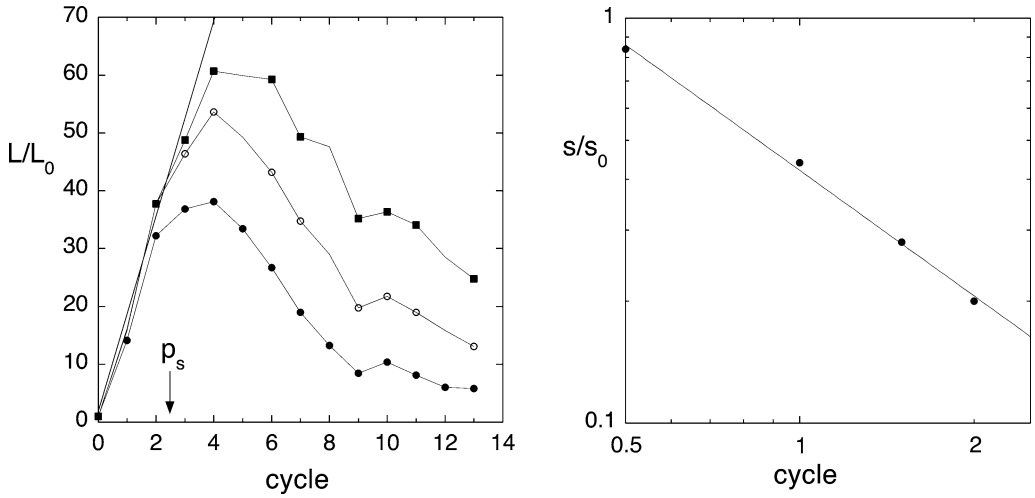

Fig. 4. Left: Contour length of the drop as it deforms through the mixing cycles for three different concentration thresholds. The length increases linearly independently of the concentration thresholds chosen to define the contour up to the mixing cycle $p_s \approx 2.5$. For $p > p_s$, the contour length depends on the concentration threshold and, at fixed threshold, decreases as p increases. Right: corresponding average transverse sheet, or striation thickness s before the mixing cycle; the line has a slope -1.

Fig. 4. Longueur du contour de la goutte déformée en fonction du nombre de cycle d'agitation et largeur transverse des bandelettes correspondante.

The maximal rate of stretch is obtained for fluid particles close to the rod trajectory, while the protocol leaves nearly unstretched fluid parcels which therefore keep a concentration close to the initial concentration as the number of cycles is increased. Concomitantly, fluid particles are brought together in the wake of the rod, and coalesce. The amplitude of the slicing movements is constant through the cycles, so that the average concentration of the dye must be conserved; these are the ingredients required for the aggregation scenario we have described to occur.

The distributions displayed on Fig. 5 are actually reasonably well described by the Gamma functions family of Eq. (3) with an average concentration $\langle C \rangle$ constant. The maximal concentration in each single scalar filament decrease as $c(0,t) \sim (t/t_s)^{-3/2}$ and the orders of the Gamma distributions consistently follow

$$n \sim (\text{number of stirring cycles})^{3/2} \tag{10}$$

in this two-dimensional flow.

As soon as a mixture is stirred in a more or less irregular manner, the addition is made at random among the levels available in the current distribution. This operation implies that the concentration distribution evolves by self-convolution and, when it actually does, gives an a-posteriori precise definition of what "random" means. As a result, the mixture composition pertains to a class of infinitely divisible distributions [11] and their evolution selects a particular route towards uniformity, which pertains to the Central Limit paradigm as it involves sums of random variables, but which does not imply, in its transient development, Gaussians. The Gamma distribution of Eq. (3), reflects more the evolution process by addition itself than the details of the initial concentration distribution *and*, its positively skewed shape with exponential tail expresses the ever present sign of the aggregation process from which it originates, that is basically a convolution of exponentials [12–15].

These skewed distributions with exponential tails are widespread in various instances including turbulent convection [16], grid turbulence [17,18], shear layers [9], randomly stirred two-dimensional flows [19–21], jets [22] or polymer solutions [23].

Recent developments on scalar turbulence [24–27] emphasize the fluctuations in the stretching induced elongation of the fluid particles, thus giving rise to a distribution of mixing times, and therefore to distributed concentrations. In this vision, the probability that a fluid element has not been stretched enough to mix is a Poisson

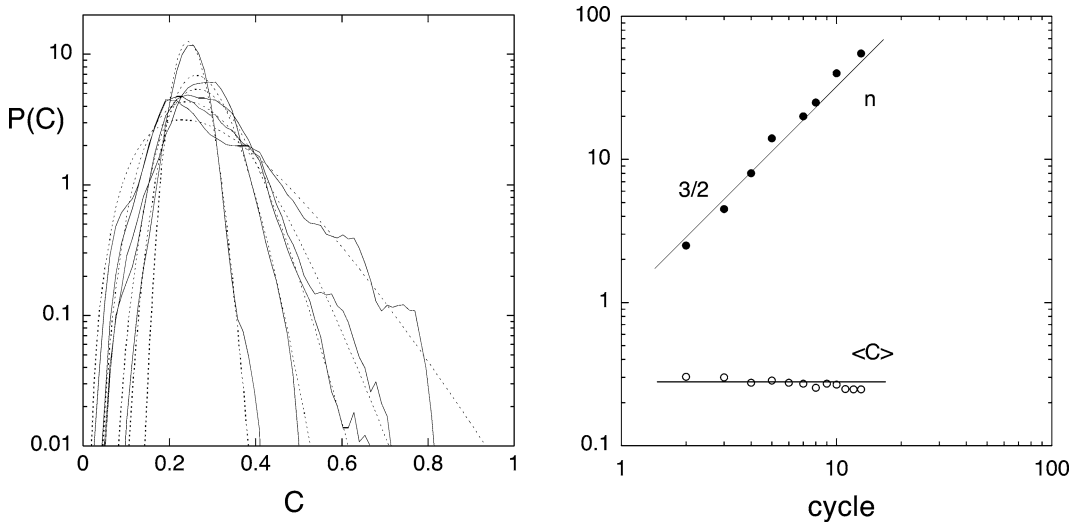

Fig. 5. Left: Evolution of the dye concentration distribution $P(C)$ after 3, 4, 5, 6 and 13 cycles according to the protocol shown on Fig. 3. The concentration distribution of the evolving mixture gets narrower around the average concentration $\langle C\rangle$. Solid line: experimental distributions, dashed line: distributions given by Eq. (3). Right: Fitting parameter n and average concentration of the distributions (3) as a function of the number of cycles.

Fig. 5. Distributions de concentration pour des nombres de cycles d'agitation croissants et ajustement par les distributions données par l'Éq. (3). Évolution du paramètre d'ajustement n en fonction du nombre de cycle.

process with a decaying exponential distribution of life, or mixing times, from which the exponential distribution of concentration follows. An alternative mechanism to build exponential tails is the aggregation scenario, at fixed mixing time. This scenario not only accounts for the distribution tails, but for their *whole* shape and evolution. The distribution of stretching histories among the fluid particles is nevertheless of importance in this mechanism. A crucial ingredient is the randomness of the interactions; it is clear the a distribution of histories, in addition to the random motions in the flow causing the addition process itself at a given instant of time, is another chance given to the decorrelation between the concentration levels being added.

To this respect, it is instructive to see that an experiment performed at a very low Reynolds number produces composition fields very similar to those obtained at much larger Reynolds number (Figs. 2 and 5). The reason is that the evolution mechanism is the same. The motion of the rod in the two-dimensional viscous fluid plays the role of the small-scale stirring motions present in high Reynolds number flows. Their role is to ensure the independence – in the statistical sense of Eq. (6) – of the addition of the concentration levels; a particularly simple paradigm for the impact of turbulence on mixing.

References

[1] J. Fourier, Théorie analytique de la chaleur, F. Didot, Père & Fils, Paris, 1822.
[2] H. Schlichting, Boundary Layer Theory, McGraw-Hill, New York, 1987.
[3] S.S. Girimaji, S.B. Pope, Material-element deformation in isotropic turbulence, J. Fluid Mech. 220 (1990) 427–458.
[4] J. Duplat, E. Villermaux, Persistency of material element deformation in isotropic flows and growth rate of lines and surfaces, Eur. Phys. J. B 18 (2000) 353–361.
[5] P.E. Dimotakis, H.J. Catrakis, Turbulence, fractals and mixing, in: H. Chaté, E. Villermaux, J.M. Chomaz (Eds.), Mixing: Chaos and Turbulence, Kluwer Academic/Plenum, New York, 1999.
[6] W.E. Ranz, Application of a stretch model to mixing, diffusion and reaction in laminar and turbulent flows, AIChE J. 25 (1) (1979) 41–47.

[7] F.E. Marble, Mixing, diffusion and chemical reaction of liquids in a vortex field, in: M. Moreau, P. Turq (Eds.), Chemical Reactivity in Liquids: Fundamental Aspects, Plenum Press, 1988.
[8] J.M. Ottino, The Kinematics of Mixing: Stretching, Chaos, and Transport, Cambridge University Press, 1989.
[9] E. Villermaux, H. Rehab, Mixing in coaxial jets, J. Fluid Mech. 425 (2000) 161–185.
[10] G.K. Batchelor, The effect of homogeneous turbulence on material lines and surfaces, Proc. Roy. Soc. A 213 (1952) 349–366.
[11] W. Feller, An Introduction to Probability Theory and its Applications, Wiley, 1970.
[12] M. von Smoluchowski, Versuch einer mathematischen Theorie der Koagulationskinetik kolloider Lösungen, Z. Phys. Chem. 92 (1917) 129–168.
[13] R.L. Curl, Dispersed phase mixing: I. Theory and effect in simple reactors, AIChE J. 9 (2) (1963) 175–181.
[14] A. Pumir, B.I. Shraiman, E.D. Siggia, Exponential tails and random advection, Phys. Rev. Lett. 66 (23) (1991) 2984–2987.
[15] S.B. Pope, Pdf methods for turbulent reacting flows, Prog. Energy Combust. Sci. 11 (1985) 119–192.
[16] B. Castaing, G. Gunaratne, F. Heslot, L. Kadanoff, A. Libchaber, S. Thomae, X.Z. Wu, S. Zaleski, G. Zanetti, Scaling of hard thermal turbulence in Rayleigh–Bénard convection, J. Fluid Mech. 204 (1989) 1–30.
[17] X. Jayesh, Z. Warhaft, Probability distributions, conditional dissipation, and transport of passive temperature fluctuations in grid-generated turbulence, Phys. Fluids A 4 (10) (1992) 2292–2307.
[18] S.T. Thoroddsen, C.W. Van Atta, Exponential tails and skewness of density-gradient probability density functions in stably stratified turbulence, J. Fluid Mech. 244 (1992) 547–566.
[19] B.S. Williams, D. Marteau, J.P. Gollub, Mixing of a passive scalar in magnetically forced two-dimensional turbulence, Phys. Fluids 9 (7) (1997) 2061–2080.
[20] M.C. Jullien, P. Castiglione, P. Tabeling, Experimental observation of Batchelor dispersion of passive tracers, Phys. Rev. Lett. 85 (17) (2000) 3636–3639.
[21] M. Holzer, E.D. Siggia, Turbulent mixing of a passive scalar, Phys. Fluids 6 (5) (1994) 1820–1837.
[22] E. Villermaux, C. Innocenti, J. Duplat, Short circuits in the Corrsin–Oboukhov cascade, Phys. Fluids 13 (1) (2001) 284–289.
[23] A. Groisman, V. Steinberg, Efficient mixing at low Reynolds numbers using polymer additives, Nature 410 (2001) 905–908.
[24] B.I. Shraiman, E.D. Siggia, Lagrangian path integrals and fluctuations in random flows, Phys. Rev. E 49 (1994) 2912–2927.
[25] B.I. Shraiman, E.D. Siggia, Scalar turbulence, Nature 405 (2000) 639–646.
[26] G. Falkovich, K. Gawedzki, M. Vergassola, Particles and fields in fluid turbulence, Rev. Mod. Phys. 73 (4) (2001) 913–975.
[27] E. Balkovsky, A. Fouxon, Universal long-time properties of Lagrangian statistics in the Batchelor regime and their application to the passive scalr problem, Phys. Rev. E 60 (4) (1999) 4164–4174.